Two Distinct Sites in Sonic Hedgehog Combine for Heparan Sulfate Interactions and Cell Signaling Functions

Shu-Chun Chang[1], Barbara Mulloy[2], Anthony I. Magee[1] and John R. Couchman[3]

[1] From the Molecular Medicine Section, National Heart & Lung Institute, Imperial College London, Sir Alexander Fleming Building, South Kensington, London SW7 2AZ, UK

[2] National Institute for Biological Standards and Control Blanche Lane, South Mimms, Potters Bar Hertfordshire, EN6 3QG,, UK

[3] Department of Biomedical Sciences, University of Copenhagen Biocenter, Ole Maaløes Vej 5, 2200 Copenhagen N, Denmark

Running title: *Sonic hedgehog-heparan sulfate interactions*

To whom correspondence should be addressed: John R. Couchman, Department of Biomedical Sciences, University of Copenhagen, Biocenter, Ole Maaløes Vej 5,2200 Copenhagen N, Denmark Tel: 0045 353 25670; E-mail: john.couchman@bric.ku.dk

Keywords: proteoglycan, morphogen, heparin, pancreatic adenocarcinoma

SUMMARY

Hedgehog (Hh) proteins are morphogens that mediate many developmental processes. Hh signaling is significant for many aspects of embryonic development, whereas dysregulation of this pathway is associated with several types of cancer. Hh proteins require heparan sulfate proteoglycans (HSPGs) for their normal distribution and signaling activity. Here we have used molecular modelling to examine the heparin-binding domain of Shh. In biochemical and cell biological assays the importance of specific residues of the putative heparin-binding domain for signaling were assessed. It was determined that key residues in hShh involved in heparin and HSPG syndecan-4 binding and biological activity included the well known cationic Cardin-Weintraub motif (lysine 32-lysine38), but also a previously unidentified major role for lysine 178. The activity of Shh mutated in these residues was tested by quantitation of alkaline phosphatase activity in C3H10T1/2 cells differentiating into osteoblasts and hShh-inducible gene expression in PANC1 human pancreatic ductal adenocarcinoma (PDAC) cells. Mutated hShhs such as K37/38S, K178S and particularly K37/38/178S that could not interact with heparin efficiently had reduced signaling activity compared to wild type hShh or a control mutation (K74S). In addition, the mutant hShh proteins supported reduced

proliferation and invasion of PANC1 cells compared with control hShh proteins, following endogenous hShh depletion by RNAi knockdown. The data correlated with reduced Shh multimerization where the K37/38 and/or K178 mutations were examined. These studies provide a new insight into the functional roles of hShh interactions with HSPGs, which may allow targeting this aspect of hShh biology in, for example, PDAC.

INTRODUCTION

Hedgehog proteins (Hhs) are morphogens that spread from producing cells to specify a diverse range of cell fates in a wide variety of tissues, in a concentration-dependent manner [1]. In mammals, all three members of the Hh family, Sonic (Shh), Indian (Ihh) and Desert (Dhh) Hedgehog, display a variety of roles in embryonic development, adult homeostasis, and cancer [2]. Perturbations to the Hh signaling pathway manifest themselves in disease; for instance, over-activity of the pathway can lead to oncogenesis while decreased activity can result in developmental malformations. It has been estimated that 25% of all human tumors require Hh signaling to maintain tumor cell viability [3]. Therefore, to establish potent Hh inhibitors and biomarkers are significant goals for diagnosis and treatment of diverse human tumors.

In vertebrates, Shh signaling regulates the development of many diverse, tissue types that includes examples of ectodermal, mesodermal and endodermal lineage [4,5]. Recent findings on Gli-stimulated transcription of cyclin B1 and cyclin D1 suggest that, through regulation of cyclin-dependent cell proliferation, the pathway is able to guide tissue specification as well as tissue maintenance [6]. Mutations in Hh pathway genes or dysregulation of the pathway are associated with certain cancers. Inappropriate Shh signaling is frequently related to tumor initiation and maintenance, e.g. basal cell carcinomas (BCCs) and medulloblastomas are often characterised by inactivation of the Shh receptor Ptc1 or constitutive activation of the signal transducer Smo [7,8], manifested as increased transcription of target genes of the Shh pathway [9]. That *Shh* acts as a dominant oncogene was shown in studies from mice and humans, in which ectopic expression of *Shh* results in BCC [10,11]. In addition, ectopic expression of *Gli1* or *Gli2* in mice results in tumor formation, indicating that activating downstream components of the pathway is sufficient to initiate tumor growth [12]. Shh signaling also plays a role in the pathogenesis of chronic myelogenous leukemia, gliomas and multiple myeloma [13-15].

Shh signaling is active during pancreatic organogenesis and low-level expression of *Hip1, Ptch1, Smo, Ihh* and *Dhh* has been detected within mature islets and cultured cell lines [16,17]. In pancreatic ductal adenocarcinoma (PDAC), the Shh signaling pathway is frequently upregulated [18]. In *in vitro* co-culture assays, the PDAC cell lines PANC-1 and ASPC-1 (which overexpress Shh) were able to activate Gli transcription in co-cultured C3H10T1/2 cells [19]. Moreover, implanting the human PDAC cell line HPAF-II into Ptc1-LacZ mice, revealed upregulated Ptc1 in the stromal cells surrounding the implant, but not in the tumor tissue. These data suggest that upregulation of Shh in PDAC cells can influence tumor growth via paracrine interactions with adjacent normal stroma. Additionally, gene expression studies in PDAC precursor lesions have demonstrated high expression levels of Shh target genes, including Gli1 and Ptc1, and cyclin D1.

Heparan sulfate proteoglycans (HSPGs) have crucial roles in many developmental signaling systems involved in cell fate determination and differentiation, interacting with members of the Wnt, Hh, transforming growth factor-β (TGF-β) and fibroblast growth factor (FGF) pathways [20]. HSPGs are extracellular matrix (ECM) and cell surface macromolecules that consist of a core protein with one or more covalently attached heparan sulfate (HS) chains. Syndecans and glypicans are two major cell surface HSPGs. Both are integral membrane proteins: syndecans are transmembrane proteins whereas glypicans are linked to the plasma membrane by a glycosylphosphatidylinositol (GPI) linkage. Perlecans are secreted HSPGs that are mainly distributed in the ECM [21]. The HS chains are the major site of interaction between proteoglycans and morphogens such as Hh, growth factors, cytokines and ECM molecules. HSPGs mediate Hh function in invertebrate and vertebrate embryos through regulation of morphogen stabilisation, release and signaling activity [20]. They are also believed to facilitate the presentation of Hh ligand to signal-receiving cells and participate in promoting cell surface microdomains/lipid rafts in which the crucial molecules are assembled into functional complexes [20].

Although dual lipidation of Hh is essential for membrane association, HSPGs also contribute to cell surface association. HSPGs may be required for multimer formation [22] and might be linked to Hh by Shifted, a secreted Wnt Inhibitory Factor homologue. The N-terminal region of Shh contains a basic motif that is conserved across vertebrates. It conforms to the Cardin-Weintraub motif (XBBBXXBX, where B is a basic residue and X is any residue) that was shown to be canonical for the interaction of some heparin-binding growth factors to heparin. In the case of human Shh, this region, consisting of residues 32-38 (with the sequence KRRHPKK) plays a role in the binding of Shh to HS. Experiments have shown that mutations in this domain are linked to a decrease in the proliferative activity induced by ShhN on cerebellar granule cell precursors, for example [23].

Here we have investigated the interaction between human (h) Shh and HSPGs through expression of mutant Shh proteins that are compromised in heparin-binding. A series of *in vitro* and cell-based assays reveal an important role for lysine 178 of Shh, as predicted from our molecular modelling of Shh-heparin interactions. This is in addition to an essential role of the cationic region between residues 32 and 38. The biological functions of purified wild-type and mutated hShhs that have reduced or negligible interaction with heparin have been tested by paracrine alkaline phosphatase induction in C3H10T1/2 cells as well as induction of Ptc and Gli1 mRNA and protein in PANC1 PDAC cells. In addition, RNAi knockdown of endogenous hShh using synthetic oligonucleotides in PANC1 cells was followed by treatment with these mutated hShhs in proliferation and invasion assays. In all cases, biological activity of Shh was markedly reduced in parallel with reduced heparin affinity. A potentially key underlying property of the mutated hShhs was shown to be markedly reduced multimerization compared to the wild type protein.

EXPERIMENTAL PROCEDURES

Modelling of Heparin/Hh and Heparin/Shh interactions - Docking calculations were performed using the program Autodock as described previously [24]. This protocol allows a simple and computationally inexpensive search of the whole protein surface for the

optimum heparin binding site, but does not predict the 'pose' of the ligand within the binding site, and does not allow for any flexibility in the protein. Two pentasaccharide structures based on the solution structure of heparin (1HPN.pdb) were used as ligands [25]; both had the sequence D-GlcNSO$_3^-$6SO$_3^-$α-(1→4)-L-IdoA2SO$_3^-$α-(1→4)-D-GlcNSO$_3^-$6SO$_3^-$α-(1→4)-L-IdoA2SO$_3^-$α-(1→4)-D-GlcNSO$_3^-$6SO$_3^-$ (abbreviated to GlcNS6S-IdoA2S-GlcNS6S-IdoA2S-GlcNS6S). The IdoA residues were set to the $^1C_4$ conformation in one of the pentasaccharides and the $^2S_0$ conformation in the other, to reflect the conformational mobility of this saccharide residue. Both of these ligands were allowed rotations around exocyclic bonds except for the glycosidic linkage bonds. A further undecasaccharide model with the sequence (GlcNS6S-IdoA2S)$_5$-GlcNS6S was also used as a ligand; in this model no bonds were allowed to rotate, the structure remaining rigid. The coordinates for mouse Shh were taken from 1VHH.pdb [26], and for human Shh from chain A of the 1.85Å crystal structure 3M1N.pdb [27].

Cell culture and Syndecan-4 purification - *C3H10T1/2* fibroblasts generously provided by Dr. Kay Grobe were maintained in Dulbecco's modified Eagle's medium (DMEM) supplemented with 8% fetal bovine serum. PANC1 cells purchased from ATCC (CRL-1469) were maintained in DMEM supplemented with 8% fetal bovine serum (FBS). Full length rat syndecan-4 cDNA in pCAGIP (28) was transfected into Cos-7 cells and stable transfectants selected over 7 days from 48h after transfection by 0.5 μg/ml puromycin. Cos-7 cells constitutively shed syndecan-4 from the cell surface, enabling purification from conditioned media. Cultures were transferred over 5-7 days into a serum-free medium (Panserin 604; PAN Biotech, Aidenbach, Germany) and medium was harvested every 3-4 days. Syndecan-4 ectodomain was purified by conventional anion exchange chromatography as described (29) and verified by western blotting. All cell cultures were routinely tested for mycoplasma contamination.

Cloning and Expression/Purification of Recombinant Shh - The human Shh cDNA clone was purchased from the I.M.A.G.E. Consortium (Accession No: BC111925, Clone ID: 40080739). To express and purify active Shh from *Escherichia coli,* pET41a(+)-ShhNC24II was constructed. Site-directed mutagenesis using the QuickChange Kit (Stratagene) was used to replace Cys24 with Ile-Ile and to add a stop codon after Gly197. In these bacterially expressed Shh proteins, the Ile-Ile replacing Cys24 is to mimic the hydrophobic nature of the N-terminal palmitoylated Cys24 of natural mammalian expressed Shh, following enterokinase-catalysed cleavage of the GST; the stop codon is to terminate the protein at the site at which it would be autocleaved mammalian cells. When expressed naturally in mammalian cells a palmitate would be added to the N-terminus and a cholesterol would be added to the C-terminus after internal autocleavage at Gly197; neither of these lipid additions takes place in bacterial cells so the bacterially expressed proteins are modified to increase the potency of the recombinant Shh proteins. This is similar to the approach taken for production of commercially available rShh (R&D Systems, Recombinant Human Sonic Hedgehog (C24II), NTerminus, Catalog Number 1845SH). Then, ShhNC24II cDNA was cloned into the pET-41a(+) expression vector at the PshAI and SacI sites to form pET41a(+)-ShhNC24II. We next generated

pET41a(+)-ShhNC24II/K37.38S, pET41a(+)-ShhNC24II/K178S, pET41a(+)-ShhNC24II/K37.38.178S and pET41a(+)-ShhNC24II/K74S by site-directed mutagenesis. *E. coli* DH5α and XL1 blue were used as competent cells for general cloning. All restriction enzymes were purchased from NEB and all PCR products were sequence-verified. Bacterial cultures of GST-ShhNC24II clones were grown overnight and induced with a final concentration of 0.1 mM isopropyl-β-D-thiogalactopyranoside (IPTG) overnight at 20 °C. Cells were harvested (4,000 × g, 30 min) then suspended in ice-cold PBS (150 mM NaCl, 2.7 mM KCl, 10 mM Na_2HPO_4, 1.8 mM KH_2PO_4, pH 7.4) and lysed in the presence of 0.2% lysozyme and 1% Triton X-100 for 30 min on ice with sonication. The extracts were centrifuged to remove the cellular debris and GST-ShhC24II fusion proteins were captured on columns of Glutathione-Sepharose 4B (GE Healthcare). Recombinant enterokinase (rEK) (S•Tag™ rEK Purification Kit, Novagen) was applied directly to the beads to release ShhNC24II proteins. Residual rEK was removed using Ekapture Agarose beads, leaving the purified 19kDa soluble ShhNC24II proteins.

To establish a mammalian overexpression system of fully-lipidated hShh, a pcDNA-DEST40-hShh expression vector was constructed using the Gateway cloning system (Invitrogen) based on recombination between an entry vector and a destination vector. pENTR223.1-hShh (DNAFORM) was propagated in *E. coli* using spectinomycin (100 μg/mL) for selection while pcDNA-DEST40 (Invitrogen) was selected by chloramphenicol (30 μg/mL) and the pcDNA-DEST40-hShh construct by ampicillin (100 μg/mL). Then, pcDNA-DEST40-hShhK37.38S, pcDNA-DEST40-hShhK178S, pcDNA-DEST40-hShh K37.38.178S and pcDNA-DEST40-hShhK74S were obtained by site-directed mutagenesis. The constructs were verified by sequencing and Western blotting of expressed Shh following transfection into PANC1 cells with Lipofectamine 2000 (Invitrogen).

Characterisation of purified human ShhNC24II protein -. Western blotting and dot blotting were carried out using both rabbit polyclonal anti-Shh (H-160; Santa Cruz Biotechnology, sc-9024) and function-blocking mouse monoclonal anti-Shh 5E1 (Developmental Studies Hybridoma bank, USA) on 50 ng of each purified protein. Secondary antibodies were horseradish peroxidase (HRP)-conjugated goat anti-mouse IgG or HRP-conjugated goat anti-rabbit IgG (Southern Biotech). Bound immunocomplexes were detected using enhanced chemiluminescence detection reagents (Pierce) and were visualised by exposing the membrane to x-ray film (Fuji medical x-ray film, Super RX, 11860). Protein concentrations were measured using Bio-Rad Protein Assay Reagent (Bio-Rad, Richmond, CA, USA) following the manufacturer's protocol. Interactions of human Shh proteins with syndecan-4 proteoglycan were assessed by dot blotting. Syndecan-4 (0-10 μg) was absorbed to the nitrocellulose membrane followed by blocking with 5% skim milk. 1 μg/μl Shh proteins (ShhNC24II, ShhNC24II/K37.38S, ShhNC24II/K178S, ShhN C24II/K37.38.178S or ShhNC24II/K74S in PBS were applied to the membrane at 37 °C for 1 h; the bound Shhs were detected with H160 antibody. In control experiments, 1 μg/μl hShh proteins were mixed with heparin (sodium salt, Sigma, 1 μg/μl) at room temperature for 15 min. The pre-incubated mixture was applied to the membrane following the procedures described

above.

Heparin binding assay - Purified wild type and mutant hShhNC24II proteins (ShhNC24II/K37.38S, ShhNC24II/K178S, ShhNC24II /K37.38.178S and ShhNC24II/K74S; 100 µg in 100 µL phosphate buffer: 2.7 mM KCl, 10 mM Na_2HPO_4 and 1.8 mM KH_2PO_4, pH 7.4) were applied to a heparin affinity column (HiTrap Heparin HP, 0.7 x 2.5 cm; GE Healthcare) using an ÄKTA system (Pharmacia LKB). Elution was with a linear gradient of 0-0.7 M NaCl that was confirmed by continuous conductivity measurement. A positive control for the chromatography, the HepII domain of fibronectin, was kindly provided by Dr. Atsuko Yoneda (University of Copenhagen). The eluates were examined by Shh dot blotting with 5E1 anti-Shh antibody. In control experiments, 10 µg ShhNC24II were applied to heparin-agarose columns with or without preincubation with 1 mg/ml heparin (sodium salt, Sigma). Binding and elution were monitored by dot blotting with 5E1 antibody.

Differentiation of C3H10T1/2 osteoblast precursor cells - alkaline phosphatase (AP) assay - Cells were plated at 1 X 10^5 per well in 6-well plates. Purified hShhNC24II proteins were added to the culture medium the day after plating at a concentration of 300, 500, 1000 or 2000 ng/ml. Monoclonal antibody 5E1 is a specific inhibitor of the Shh pathway by binding to Shh and neutralising its activity [30]. To some samples, 5E1 (10 µg/ml) was added together with hShh proteins. Five days after treatment, C3H10T1/2 cells were lysed (in 150 µl 1% Triton X-100 in PBS, pH 7.4 with complete protease inhibitor cocktail (Roche) and Shh activity was tested by measuring alkaline phosphatase induction in the cells at 405 nm using a microplate reader (Bio-Rad Lumimark), accomplished by incubation with 150 µl 120 mM *p*-nitrophenol phosphate (Sigma), 50 mM $MgCl_2$ and 1 M diethanolamine (Sigma) at room temperature for 30 min. Assays were performed in triplicate.

Semi-quantitative Reverse Transcription-PCR - After treatment with 1µg/ml purified proteins (ShhNC24II, ShhNC24II/K37.38S, ShhNC24II/K178S, ShhNC24II/K37.38.178S or ShhNC24II/K74S) for 24 h, PANC1 cells were analyzed by Reverse Transcription-PCR (RT-PCR). Total RNA extraction with Trizol (Invitrogen) was followed by cDNA synthesis by random priming of 1µg of total RNA with SuperScript II Reverse Transcriptase kit (Invitrogen), according to the manufacturer's instructions. The following primers were used for the subsequent PCR: human *GAPDH* (sense, 5'-TTCATTGACCTCAACTACAT-3'; antisense, 5'-GTGGCAGTGATGGCATGGAC-3'); human β-*actin* (sense, 5'-ATGGATGAGGATATCGCTGCG-3'; antisense, 5'-CTAGAAGCATTTGCGGTGCAC-3'); human *Shh* (sense, 5'-CGCACGGGGACAGCTCGGAAGT-3'; antisense, 5'-CTGCGCGGCCCTCGTAGTGC-3') [31]; human *Ptc* (sense, 5'-GGTGGCACAGTCAAGAACA-3'; antisense, 5'-ACCAAGAGCGAGAAATGG-3') [31]; human *Smo* (sense,5'-TTACCTTCAGCTGCCACTTCTACG-3'; antisense, 5'-GCCTTGGCAATCATCTTGCTCTTC-3') [32]; human *Gli1* (sense, 5'-TTCCTACCAGAGTCCCAAGT-3'; antisense, 5'-CCCTATGTGAAGCCCTATTT-3') 32].

PCR with Taq DNA Polymerase (Invitrogen) used the following conditions: 30 cycles of 30 s at 95° C, 30s at 60° C, and 2min/kb at 72° C. PCR products were resolved by electrophoresis on 1.7% agarose gels and visualised by ethidium bromide staining.

Functional assay of hShh proteins in PANC1 cells: Western blotting. Four h after plating PANC1 cells (3 X 10^5 cells per well in a 6-well plate), 1μg/ml purified hShh proteins (ShhNC24II, ShhNC24II/K37.38S, ShhNC24II/K178S, ShhNC24II/K37.38.178S and ShhNC24II/K74S) with or without 5E1 antibody (10 μg/ml) were added to the culture medium. Cells were harvested 48 h later and analyzed by Western blotting. Goat polyclonal anti-patched (Ptc; ab51983) and mouse monoclonal α-tubulin (DM1A, ab49928) were from Abcam, while rabbit polyclonal anti-Gli-1 (H-300, sc-20687) was purchased from Santa Cruz Biotechnology. Secondary antibodies were HRP-conjugated goat anti-mouse IgG, HRP-conjugated goat anti-rabbit IgG or HRP-conjugated donkey anti-goat IgG (Southern Biotech). Bound immunocomplexes were detected using enhanced chemiluminescence detection.

Human (h)Shh RNAi knockdown -. Human Shh siRNA pooled oligomers (sc-29477) were from Santa Cruz Biotechnology, Inc. The negative control was SilencerR FAMTM-Labelled Negative Control #1 siRNA (Ambion). siRNA transfections were carried out with FuGENE 6 Transfection Reagent (Roche) by plating 0.3 million cells per well in a 6-well plate and 6 h later treating with 10 pmol siRNA oligomers and 3 μl FuGENE 6 Transfection Reagent. Western blots and dot blots of conditioned media were analyzed and quantitated by densitometry to assess the extent of Shh reduction. Immunoblotting was carried out using rabbit polyclonal anti-Shh H-160 on cultures harvested 24 h, 48 h and 72 h after siRNA transfection.

Shh oligomerisation assay - In these assays, siRNA treatment to knock down endogenous Shh and plasmid transfection for wild type or mutant Shh protein expression were carried out sequentially in PANC1 cells. PANC1 at 1 x 10^5 cells/well in a 6-well format (2 ml medium, no antibiotics) were treated with 10 pmol of Shh siRNA with FuGENE 6 transfection agent (as above) to knock down endogenous wild type Shh. After 16 h, pcDNA-DEST40-hShh expression vectors were transfected into the cell and 72 h after siRNA transfection, culture medium was changed to serum-free medium for 24 h. Conditioned media were collected, clarified by and centrifugation and analyzed by gel filtration chromatography (ÄKTA Protein Purifier, Amersham Biosciences) on a Superdex 200 10/300 GL column (Amersham Biosciences) equilibrated with phosphate buffer, detailed above, at 4° C. The molecular mass standards Blue dextran, 2000kDa; Apoferritin, 480 kDa; Alcohol dehydrogenase, 150 kDa; Albumin, 67 kDa and recombinant Human ShhN (C24II) (R&D Systems, Inc.), 19 kDa were used to calibrate the column. Eluted fractions (1 ml) were collected, trichloroacetic acid (TCA)-precipitated, then assayed by dot blotting with H-160 Shh antibody.

PANC1 invasion assay - Biocoat Matrigel invasion chambers with 8 μm pores in 6-well plates (BD Biosciences) were used in invasion assays. To determine the effect of mutated Shh proteins on PANC1 invasion ability, 72 h before PANC1 cells were plated to the chambers the cells were pretreated with hShh siRNA reagent together with exogenous recombinant Shh proteins (1 μg/ml). Shh proteins-containing media were changed every 48 h. PANC1 cells were detached with 5mM

EDTA in PBS. Detached cells were resuspended in serum-free DMEM and added to the upper compartment of the chambers (1 X 10^5 cells/well). Conditioned medium (8% FBS) was placed in the lower chambers. After 24h of incubation at 37° C, the cells on the upper surface were completely removed by wiping with a cotton swab, and then the filter was fixed with 100% methanol and stained with crystal violet solution (0.5% (w/v) crystal violet in 25% (v/v) methanol). Cells that had migrated from the upper to the lower side of the filter were photographed and counted with a light microscope (10 fields/filter).

PANC1 proliferation and flow cytometry - Proliferation was measured with the vital dye carboxyfluorescein diacetate, succinimidyl ester (CFSE ; Sigma). The essence of this assay is that cells are loaded with dye that becomes successively diluted by division into daughter cells at each mitosis. Briefly, after 24 h of synchronization in serum-free medium, cells were treated with hShh siRNA together with purified hShh proteins (1 μg/ml each hShhNC24II, hShhNC24II/K37.38S, hShhNC24II/K178S, hShhNC24II/K37.38.178S or hShhNC24II/K74S), or 5E1 blocking antibody (10 μg/ml) separately, and cells were labelled with 2.5μM CFSE at 37° C for 15 min. Shh proteins-containing media were replenished every 48 h. In some cases, 5E1 antibody treatment was carried out 72 h after synchronization, to mimic siRNA KD kinetics. After 8 days stimulation, cell division was indicated by decreased CF fluorescence intensity per cell, as analyzed by flow cytometry. For flow cytometer assessment, PANC1 cells were removed from plates with ice-cold FACS buffer (1% FBS and 2 mM EDTA in PBS) and resuspended in the same buffer. Cells were analyzed with a FACScalibur flow cytometer.

Statistical analysis -. All experiments were replicated at least three times, and statistical significance was measured by using the two-tailed t test. A p value <0.05 was taken to indicate statistical significance. All target signals from Western blots and dot blots were quantified by Scion Image software.

RESULTS

Molecular Modelling of Shh–heparin interactions. The crystal structure of mouse Shh (1VHH.pdb) is truncated at the N-terminus, starting at K39 (the equivalent of K38 in the human sequence). Docking calculations for both pentasaccharides and undecasaccharides indicated that the optimum heparin-binding site involves this N-terminal residue (Fig. 1A), and in addition, residue K179 distant in the sequence (K178 in the human sequence). A structure of human Shh (1M1N.pdb) has also been determined, that retains more of the N-terminal sequence which does not form part of the globular structure but adopts an extended structure stabilized by crystal contacts. This N-terminal sequence contains several basic residues, and docking to this structure indicates that residues R28, K32 and K34 can form a heparin-binding site independently of the globular, structured protein (Fig. 1B). This was the case not only for the relatively short, partly flexible pentasaccharide ligands, but also for the extended and rigid undecasaccharide structure. As the protein structure is rigid in the docking protocol used [24], the extended conformations of the N-terminal sequences in 1VHH.pdb and 1MIN.pdb are retained in the final models of the docked complexes, which may well not be an accurate reflection of their behaviour in solution.

This raised the question of whether the distant K179 identified in the truncated murine Shh structure is a genuine part of the heparin-binding site of Shh, or is an artefact of the docking calculation. To address this, specific mutations in human Shh, including that of K178 were carried out for a series of biological assays.

*Characterisation of purified human Sonic Hedgehog (hShh) proteins***.** To examine the folding of mutated hShh proteins purified from *E. coli*, two different hShh antibodies, 5E1 (a Shh neutralizing antibody recognizing the active site) and H-160, were used in Western blotting (Fig. 2A) and dot blotting (Fig. 2B). The 5E1 antibody was used to define the degree of native folding of purified hShh proteins [33]. Similar reactivity of wild type and mutant forms of the Shh proteins to 5E1 in dot blots suggests that they are all correctly folded to a similar degree. The H-160 antibody was used as a loading control.

Lysine 37/38 and lysine 178 of hShh play crucial roles in interactions with heparin and HSPG. Previous studies in *Drosophila* [34] and vertebrate systems [35] suggested that by forming a multimeric complex with specific HSPGs - perlecan and glypican – the efficiency of Shh signaling could be facilitated. To confirm that hShhNC24II could interact with heparin, we initially used a small scale heparin affinity assay and verified the specificity in the presence of competing free heparin (data not shown). Next, to determine the key residues on hShh involved in heparin binding, affinity chromatography on a heparin-agarose column with gradient salt elution was employed. In this assay, wild type (ShhNC24II) and mutated recombinant hShh proteins ShhNC24II/K37.38S, ShhNC24II/K178S, ShhNC24II/K37.38.178S and ShhNC24II/K74S) were analyzed with elution by a 0 to 0.7 M NaCl gradient (Fig. 2C). The results showed that ShhNC24II had a peak elution at 0.54 M NaCl which was similar to ShhNC24II/K74S (0.53 M NaCl), whereas ShhNC24II/K37.38S and ShhNC24II/K178S exhibited reduced heparin affinity, being eluted at 0.4 M NaCl and 0.3M NaCl, respectively). The triple mutant, ShhNC24II/K37.38.178S was essentially lacking in heparin binding (n=5), suggesting that not only lysine residues 37 and 38 (of the previously identified Cardin-Weintraub motif) but also lysine178 of hShh play critical roles in heparin, and presumably HSPG, binding. Moreover, lysine 74 plays no part in binding to heparin, verifying that this mutation serves as a negative control.

In further dot blotting experiments with syndecan-4 ectodomain, which is substituted with HS chains, similar data were obtained as seen with heparin interactions. Wild type ShhNC24II and ShhNC24II/K74S bound to the proteoglycan, in a manner sensitive to heparin competition (Supplementary Fig. 1). The triple mutant ShhNC24II/K37.38.178S bound poorly, while the ShhNC24II/K37.38S and ShhNC24II/K178S forms were intermediate (Supplementary Fig. 1). Therefore, it appears that K178 contributes substantially to interactions with HSPGs (at least syndecan-4) as well as free heparin glycosaminoglycan.

Bioactivity of mutated hShhs in C3H10T1/2 cells: heparin-binding is required to induce alkaline phosphatase activity. To examine the biological functions of the different hShhNC24II proteins, the C3H10T1/2 osteoblast precursor cell line was utilized, which expresses alkaline phosphatase (AP) when stimulated by Shh [22]. As shown in Fig. 3A, both ShhNC24II- and ShhNC24II/K74S-supplemented medium (1 μg/ml) induced C3H10T1/2 differentiation into

AP-producing osteoblasts, demonstrating competent biological activity of these purified hShh proteins. Lysine 74 mutation to serine had no impact in this assay. In contrast, ShhNC24II/K37.38S and ShhNC24II/K178S were reduced by 50-75% in their activity in the assay (Fig. 3A). Of note, the single K178S mutant Shh protein gave a greater reduction in AP expression than the K37/38S mutant compared to the wild type protein. Moreover, the ShhNC24II/K37.38.178S triple mutant exhibited a further reduction in AP induction. However, when hShh proteins were increased to 2 μg/ml the differences in AP activity between them decreased, but remained statistically significant (Fig. 3A). To verify whether the induced AP activity was due directly to the hShh proteins, we used Shh-neutralising antibody 5E1 [33] as a specific inhibitor of Shh-induced C3H10T1/2 differentiation (Fig. 3B). The biological activity of Shhs was significantly inhibited by 5E1 co-treatment. In summary, these data show that ShhNC24II/K37.38S, ShhNC24II/K178S and particularly ShhNC24II /K37.38.178S mutants are greatly reduced in their ability to bind heparin and to induce osteoblast differentiation. High doses of recombinant Shh proteins were required in this assay, consistent with the lack of post-translational lipid modifications of the bacterially expressed proteins.

*ShhNC24II/K37.38.178S fails to stimulate signaling through the Shh pathway in PANC1 cells.*To further study the signaling activity of mutated Shhs, semi-quantitative reverse transcription-polymerase chain reaction (RT-PCR) and Western blots for proteins that represent Shh target genes were performed on PANC1 cells pre-treated with 1 μg/ml hShhs for 24 or 48 h. Therefore, the signaling activity obtained from both assays was a consequence of endogenous hShh plus exogenous purified Shh proteins in PANC1 cells. Previous studies reported that Shh responses are mediated primarily by the transcription factors Gli1, Gli2, Gli3 [12] and the receptor Ptc. Unlike Gli2 and Gli3, which can function as either transcriptional activators or repressors, Gli1 only functions as an activator, and only one isoform of Gli1 has been identified. In RT-PCR (Fig. 4A, B), GAPDH and β-actin were used as controls. In comparison with untreated cells, 5E1 treatment strongly reduced both Ptc and Gli1 expression by 70% and 79% respectively. On the other hand, compared to ShhNC24II and ShhNC24II/K74S positive controls, ShhNC24II/K37.38S and ShhNC24II/K178S both failed to increase Ptc and Gli1 (mRNA levels for Ptc and Gli1 were decreased by >20% and >25% respectively, $P<0.001$), whereas Shh and Smoothened (Smo) mRNA levels were unchanged. More importantly, ShhNC24II/K37.38.178S addition resulted in further reduction in Ptc and Gli1 by >28% and >47% respectively compared with ShhNC24II treated cells ($P<0.001$).

Immunoblotting was carried out to confirm the RT-PCR results (Fig. 4C, D). In Western blots for Ptc, both ShhNC24II/K178S and ShhNC24II/K37.38.178S addition led to marked reduction in protein levels by 44% and 60% respectively ($P<0.001$), compared to ShhNC24II- and ShhNC24II/K74S-treated cells. In addition, less Gli1 was induced in response to ShhNC24II/K178S and ShhNC24II/K37.38.178S with 53% and 57% reduction respectively ($P<0.005$) compared to ShhNC24II and ShhNC24II/K74S proteins. Therefore, modifications of wild type Shh affecting potential HSPG binding sites (K37, 38 and 178) resulted in a large reduction in the activity in both C3H10T1/2 and PANC1 assays

(Figs. 3 and 4), suggesting that HSPG interactions are essential for Shh signaling in these cell systems. Mutation of either the K37/38 or of K178 reduced activity significantly and to a comparable degree. However, mutation of all three lysine residues was required for almost complete inactivation of Shh biological activity, suggesting that they contribute additively to HS interactions.

*Mutant Shh with reduced heparin affinity cannot rescue inhibition of PANC1 proliferation caused by endogenous hShh depletion.*A dependency of PANC1 proliferation on Shh was demonstrated by treating cells with the inhibitory Shh antibody 5E1. The data show that carboxyfluorescein (CF) intensity after 8 days in culture of cells treated with 5E1 on day 1 was ~30 times higher than untreated cells (Fig. 5), suggesting that untreated PANC1 cells replicate 4-5 times more than 5E1-treated cells over 8 days. Moreover, cells treated with 5E1 from day 4 (used to mimic Shh siRNA kinetics) contained ~8 times higher CF intensity compared to untreated cells. Both results support the interpretation that PANC1 proliferation is Shh-dependent. Knockdown (KD) of Shh by siRNA treatment gave similar results to the use of 5E1 antibody from day 4. Western blots confirmed >90% Shh depletion after siRNA (Supplementary Fig. 2). A scrambled siRNA used as a negative control showed similar CF fluorescence levels to untreated cells.

In a background of endogenous Shh depletion (denoted Shh KD), PANC1 cells were exposed to wild type or mutant Shh proteins. Flow cytometry profiles of Shh KD cells treated with either ShhNC24II/Shh or ShhNC24II/K74S yielded similar results to untreated cells (mean fluorescence intensity; MFI <1000, Fig. 5), suggesting that both ShhNC24II and ShhNC24II/K74S proteins are able to rescue reduced PANC1 proliferation caused by Shh depletion (P<0.001). In contrast, purified ShhNC24II/K37.38S and ShhNC24II/K178S proteins added to culture medium showed less ability to rescue PANC1 proliferation caused by endogenous Shh KD, with ~6 times increased MFI compared to untreated cells (P<0.001). Furthermore, ShhNC24II/K37.38.178S-treated Shh KD cells showed a similar result to Shh KD cells alone, with ~8 times increased MFI compared to untreated cells (P<0.001), indicating that ShhNC24II/K37.38.178S is defective in stimulating PANC1 proliferation in comparison to ShhNC24II and ShhNC24II/K74S. These results suggest that HS binding plays an important role in PANC1 proliferation through Shh signaling since ShhNC24II or ShhNC24II/K74S could rescue inhibited PANC1 caused by hShh RNAi KD, but the triple lysine mutant ShhNC24II/K37.38.178S was unable to do so.

Mutant Shh proteins with reduced heparin affinity do not promote PANC1 invasive behavior. To investigate the contribution of Shh to invasive potential of PANC1 cells, we carried out invasion assays with exogenous Shhs treatment combined with endogenous Shh RNAi KD. To confirm that PANC1 invasion is dependent on Shh signaling, the effect of 5E1 treatment on PANC1 invasion was determined. The results (Fig. 6) showed a significant decrease in the number of invading cells after 5E1 treatment (33±8 cells/well) compared with untreated control cells (271±25 cells/well). These data were then verified by Shh KD which resulted in migration of 43±11 cells/well. These results suggested that the invasive ability of PANC1 cells was at least partly a result of autocrine Shh signaling. When endogenous Shh depletion and either ShhNC24II or ShhNC24II/K74S were

combined in the invasion assay, a significant increase in the number of invasive PANC1 cells was observed (325±32 and 302±45 cells/well respectively) compared to Shh KD alone, suggesting that ShhNC24II and ShhNC24II/K74S could restore inhibited PANC1 invasion. In contrast, ShhNC24II/K37.38S and ShhNC24II/K178S combined with Shh KD showed a significant decrease in the number of invasive PANC1 cells with 192±15 and 191±18 cells/well respectively (Fig. 6). Furthermore, ShhNC24II/K37.38.178S combined with Shh KD reduced invasion to a level (86±17 cells/well) similar to that observed for Shh KD cells, indicating that ShhNC24II/K37.38S, ShhNC24II/K178S and particularly ShhNC24II/K37.38.178S provided less stimulus for PANC1 invasion. It should be noted that invasion assays over 24 h, such as this, can be influenced by proliferation. However, we found the doubling time for PANC1 cells to be ~51 h (data not shown), which cannot explain the clear effects of Shh proteins on migratory behavior. Therefore, HSPGs appear to play a crucial role in PANC1 invasion mediated by Shh signaling.

ShhNC24II /K37.38.178S is defective in forming multimeric complexes in PANC1 cells. Interaction with HSPGs has been suggested to be essential for the formation of Shh multimeric complexes [34,35]. To assess multimer formation, PANC1 cells were depleted of endogenous Shh by siRNA treatment, followed by transfection with vectors encoding wild type or mutant Shh. In this system dual lipidation of the Shh will occur, which may be essential for multimer formation. To evaluate the ability of mutated hShhs to form multimeric complexes, gel filtration followed by Shh dot blotting of each fraction were carried out for PANC1 cell conditioned media. A 19 kDa polypeptide and a large pool of high molecular mass complexes were observed in control cell media (Fig. 7). Higher levels of secreted Shh were found in medium from both untreated cells and scrambled RNAi-treated cells than from Shh KD cells, providing evidence that Shh KD reduced Shh expression. The majority of secreted Shh in PANC1 control untreated culture medium forms large complexes and only a small portion of Shh migrates as monomers (2.6±1.2%), confirming the results of a previous study [22]. In contrast, in Shh RNAi-treated cultured medium the total amount of Shh was much reduced (>90% reduction compared with untreated control cells) and higher quantities of Shh monomers were detected (12.7±4.5%, $P<0.001$), nearly 6 times higher than untreated control medium, whereas media from scrambled siRNA-treated cells showed a similar pattern to control media with 1.9±1.3% monomer. Wild type Shh or ShhK74S expression in PANC1 cells combined with Shh KD treatment, either made no difference in the proportion of monomeric versus large Shh-containing complexes, or a slight decrease in Shh monomerisation (1.2±0.9% and 1.1±0.8% respectively). Therefore, ectopically expressed wild type and K74S Shh were capable of forming complexes. Analysis of media from hShhK37.38S -expressing and hShhK178S-expressing Shh KD cells resulted in increased monomerisation, 25.5±5.7% and 20.4±4.6% respectively, ($P<0.001$). Notably, a further increase in the proportion of monomers was detected in ShhNC24II/K37.38.178S-expressing Shh KD cells (85.5±9.7%, $P<0.001$). In combination, we conclude that wild type hShh and hShhK74S form large complexes when expressed in PANC1 cells, but hShhK37.38.178S does not, while the

hShhK37.38S and hShhK178S mutants were intermediate.

DISCUSSION

Based on developmental and biochemical studies in *Drosophila* and vertebrate systems there are several proposed mechanisms for HSPG promotion of Hh signaling. On one hand, Shh and Hh are secreted from cells as both monomeric and multimeric forms. Soluble Hh multimeric complexes with HSPGs are potentially freely diffusible, which can facilitate Hh bioavailability. On the other hand, the interaction between HSPGs and Shh may influence both Shh extracellular distribution and ability to signal as shown by perlecan's ability to function as a Shh co-receptor [34]. Furthermore, HSPGs potentially participate in promoting cell surface microdomains/lipid rafts where the crucial molecules are assembled into functional complexes [36]. In this regard, the GPI-anchored glypican HSPGs may be particularly important. Therefore, HSPGs appear to facilitate Shh signaling cascades at various levels, including secretion, retention and stabilisation of ligands, directed trafficking and targeting to ligand-receiving cells.

In this report, the heparin-binding properties of Shh were examined in detail. Previously a single motif, comprising a conserved XBBBXXBX sequence, where B is a basic residue, and X is any residue, was identified in Shh [37]. This region (K32-K38) precisely coincides with a consensus sequence for heparin binding, known as the Cardin-Weintraub motif [23]. Much data have subsequently been compiled showing that this is only one of a number of cationic sequences that can bind glycosaminoglycans [38]. The importance of the K32-K38 region in Shh for binding heparin and HS has been demonstrated [38]. Our molecular modelling of murine Shh, on the other hand, suggested that another lysine residue K179 on the surface of Shh (K178 in the human sequence) may also contribute to overall affinity of the morphogen for heparin. This model included an incomplete flexible N-terminal domain, while a second model of human Shh, with a longer N-terminal region, suggested that the cationic K32-K38, with R28, formed the dominant heparin-binding motif. The hypothesis that K178 of hShh was significant for interaction with heparin, and HSPGs, was tested here. Our data support a key role for K178 in several different assays of hShh function.

First, it is apparent that mutation of two of the four lysine residues to disrupt the Cardin-Weintraub motif (K37 and K38) does not ablate heparin binding, as shown by affinity chromatography. Only when lysine 178 is additionally mutated, does heparin affinity become negligible. Very similar data were obtained from interactions with syndecan-4 proteoglycan. Entirely consistent with these binding data, several biological assays, including osteoblast differentiation, and PDAC cell proliferation and invasion also showed the same trend. Alkaline phosphatase secretion by C3H10T1/2 cells was reduced where K37 and K38 were mutated to serine residues, but was reduced much further by additional K178 mutation. Moreover, mutation of K178 alone had considerable effect, not dissimilar to the K37/K38 mutation. The same principles were noted for PANC1 proliferation and invasion of matrigel. The triple mutant was reduced four-fold in invasion-supporting activity compared to the wild type morphogen.

Multimerization of Shh is known to be a key facet of its biological function, and interaction with heparinoids is a promoter of this process, as is the dual lipidation of the protein [20]. Shh secreted from PANC1 cells

transfected with cDNAs encoding the same range of mutations, in a background of endogenous Shh depletion achieved by siRNA, was analyzed by gel filtration. Consistent with the cell biological experiments, it was noted that increasing proportions of the Shh were monomeric as the affinity for heparin declined. The triple mutant form of Shh (K37/38/178S) was largely monomeric. All this suggests that the quaternary structure and biological properties of Shh depend to a significant degree on binding of HSPGs. Therefore, given that the Cardin-Weintraub motif, while important, does not comprise the sole heparin-binding sequence of Shh, previous data can be re-evaluated. For example, work in mice has shown that a R34A/K38A mutation in Shh reduced (but did not ablate) proteoglycan affinity, but did not alter Ptc affinity [38]. Moreover, while the mutant Shh had reduced ability to promote proliferation, neuronal tissue patterning was not affected. It would be interesting to determine whether additional mutation of K178 would affect this outcome. Our data are, on the other hand, consistent with a role for HSPGs in the potentiation of Shh trafficking and targeting to receiving cells. Previous studies using mutations in the glypican Dlp, mutations in the *Ext* gene family of HS polymerases and truncation of the Cardin-Weintraub motif have suggested that HSPGs are critical for appropriate localization of Hh proteins [39,40].

The data presented here suggest that a previously unrecognised lysine residue, K178, is a key component of the heparin-binding site of human Shh. Moreover, this residue appears to be highly conserved across an array of vertebrates, from fish to amphibians, birds and mammals, including primates, as is the more well known K32-K38 motif. Molecular modelling that was used to identify K178 as a key residue in heparin binding also indicated that K74 was not, and our data substantiate this hypothesis. Mutation of K74 to serine was silent in terms of all biochemical and cell biological assays examined here, the protein being essentially indistinguishable from the wild type. Therefore, while the molecular modelling of the murine sequence correctly predicted a role for K179, that of the human Shh did not. It is probably relevant that predicting heparin-binding sequences of flexible, relatively unstructured protein regions from docking calculations can be challenging. The longer, human Shh contained more cationic residues than the murine protein, and these dominated the predicted interactions. It is revealing that the shorter murine Shh appears to have offered a physiologically relevant insight into hShh-HSPG interactions, borne out by the studies reported here.

A number of Shh responsive genes have been identified, including genes that are involved in proliferation and tissue patterning e.g. *Gli2*, *N-myc*, *Gli3*, *Cyclin D1*, *Cyclin D2* and *Bmi-1*. In addition, it has also been shown that *Cyclin D1*, *Cyclin D2* and *Bmi-1* gene targets that require Shh-HSPG interactions are significant in tumor stem cell biology [41,42]. Also, it is interesting to note that Shh-dependent cancer growth can be stimulated through glypican overexpression in several cases, e.g. prostate cancer, PDAC and rhabdomyosarcoma [43,44]. In this work, we asked whether interactions with HSPGs can modulate the pattern of Shh-responsive gene induction and the biological responses to Shh in PDAC cells. We employed mAb 5E1 to block the Shh signaling pathway in PANC1 cells, resulting in a significant decrease in proliferation (4-5 times lower over 8-days) and an eight-fold reduction in invasiveness, suggesting that Shh signaling has a critical and central role in PDAC cell

growth and contributes to malignant transformation. We directly demonstrated that K37.38S or K178S mutant results in reduced proliferation compared to wild type Shh; an even more marked effect was noted with the K37.38.178S triple mutant. We also observed a ~40% decrease in invasive cells by K37.38S or K178S treatment compared to wild-type Shh and control K74S mutant. Not surprisingly, the triple mutant K37.38.178S resulted in a four-fold reduction in invasive cells compared with wild-type Shh or control K74S mutant. Together, these findings suggest that Shh-HSPGs interactions promote PANC1 cells' oncogenic properties at multiple levels, including both proliferation and invasion, highlighting the widespread significance of proteoglycans in tumorigenesis and also pointing out an important mediator of the malignant behavior of human PDAC cells.

REFERENCES

1. Ingham, P.W. and McMahon, A.P. (2001) *Genes Dev*. **15**, 3059–3087
2. Nybakken, K. and Perrimon, N. (2002) *Curr. Opin. Genet. Dev*. **12**, 503-511
3. Briscoe, J. and Thérond, P. (2005) *Dev. Cell* **8**, 143-151
4. Bhardwaj, G., Murdoch, B., Wu, D., Baker, D., Williams, K., Chadwick, K., Ling, L., Karanu, F. and Bhatia, M. (2001) *Nat. Immunol*. **2**, 172–180
5. Doles, J., Cook, C., Shi, X., Valosky, J., Lipinski R. and Bushman, W. (2006) *Dev. Biol*. **295**, 13–25
6. Morton, J. P. and Lewis, B. C. (2007) *Cell Cycle* **6**, 1553–1557
7. Wolter, M., Reifenberger, J., Sommer, C., Ruzicka, T. and Reifenberger, G. (1997) *Cancer Res*. **57**, 2581–2585
8. Xie, J., Murone, M., Luoh, S. M., Ryan, A., Gu, Q., Zhang, C., Bonifas, J. M., Lam, C. W., Hynes, M., Goddard, A., Rosenthal, A., Epstein, E. H. Jr. and de Sauvage, F. J. (1998) *Nature* **391**, 90–92
9. Rubin, L. L. and de Sauvage, F. J. (2006) *Nat. Rev. Drug Discovery* **5**, 1026–1033
10. Oro, A. E., Higgins, K. M., Hu, Z., Bonifas, J. M., Epstein, E. H. Jr. and Scott, M. P. (1997) *Science* **276**, 817–821
11. Fan, H., Oro, A. E., Scott, M. P. and Khavari, P. A. (1997) *Nature Med*. **3**, 788–792
12. Nilsson, M., Undèn, A. B., Krause, D., Malmqwist, U., Raza, K., Zaphiropoulos, P. G. and Toftgård, R. (2000) *Proc. Natl. Acad. Sci. USA*. **97**, 3438–3443
13. Zhao, C., Chen, A., Jameieson, C. H., Fereshteh, M., Abrahamsson, A., Blum, J., Kwon, H. Y., Kim, J., Chute, J. P., Rizzieri, D., Munchhof, M., Vanarsdale, T., Beachy, P. A. and Reya, T. (2009). *Nature* **458**, 776–779
14. Clement, V., Sanchez, P., de Tribolet, N., Radovanovic, I. and i Altaba, A. R. (2007). *Curr. Biol.* **17**, 165–172
15. Peacock, C. D., Wang, Q., Gesell, G. S., Corcoran-Schwartz, I. M., Jones, E., Kim, J., Devereux, W. L., Rhodes, J. T., Huff, C. A., Beachy, P. A., Watkins, D. N. and Matsui, W. (2007) *Proc. Natl. Acad. Sci. USA.* **104**, 4048–4053
16. Thomas, M. K., Rastalsky, N., Lee, J. H. and Habener, J. F. (2000) *Diabetes* **49**, 2039–2047
17. Kawahira, H., Ma, N. H., Tzanakakis, E. S., McMahon, A. P., Chuang, P. T. and Hebrok, M. (2003) *Development* **130**, 4871–4879
18. Morton, J. P., Mongeau, M. E., Klimstra, D. S., Morris, J. P., Lee, Y. C., Kawaguchi, Y., Wright, C., Hebrok, M. and Lewis, B. C. (2007) *Proc. Natl. Acad. Sci. USA*. **104**, 5103–5108
19. Yauch, R. L., Gould, S. E., Scales, S. J., Tang, T., Tian, H., Ahn, C. P., Marshall, D., Fu, L., Janaurio, T., Kallop, D., Nannini-Pepe, D., Kotkow, K., Marsters, J. C., Rubin L. L., and de Sauvage, F. J. (2008) *Nature* **455**, 406–410
20. Lin, X. (2004) *Development* **131**, 6009-6021
21. Whitelock, J.M., Melrose J. and Iozzo R.V. (2008) *Biochemistry* **47**, 11174-11183
22. Dierker, T., Dreier, R., Petersen, A., Bordych, C. and Grobe, K. (2009) *J. Biol. Chem*. **284**, 8013-8022
23. Rubin, J. B., Choi, Y. and Segal, R. A. (2002) *Development* **129**, 2223–2232
24. Mulloy, B. and Forster, M.J. (2008) *Molec. Simulations* **34**, 481-489
25. Mulloy, B., Forster, M.J., Jones, C. and Davies, D.B. (1993) *Biochem. J.* **293**, 849-858
26. Hall, T.M., Porter J.A., Beachy P.A. and Leahy D.J. (1995) *Nature* **378**, 212-216
27. Pepinksy R.B., Rayhorn, P., Day E.S., Derga, A., Williams, K.P., Galdes A., Taylor F.R.,

Boriak-Sjodin P.A. and Garber E.A. (2000) *J. Biol. Chem.* **275**, 10995-11001
28. Alexopoulou A., Couchman, J.R. and Whiteford, J.R. (2008) *BMC Cell Biol*. **9**, 2
29. Woods, A. and Couchman, J.R. (2001) *Curr. Protoc. Cell Biol.* Ch. 10, 10.7
30. Maun, H.R., Wen, X., Lingel, A., de Sauvage, F.J., Lazarus, R.A., Scales, S.J. and Hymowitz, S.G. (2010) *J. Biol. Chem.* **285**, 26570-26580
31. Turner, T. T., Bomgardner, D. and Jacobs, J. P. (2004) *J. Androl.* **25**, 514-522
32. Feng, Y.Z., Shiozawa, T., Miyamoto, T., Kashima, H., Kurai, M., Suzuki, A. et al. (2007) *Clin. Cancer Res.* **13**, 1389-1398
33. Ericson, J., Morton, S., Kawakami, A., Roelink, H. and Jessell, T. M. (1996) *Cell* **87**, 661–673
34. Park, Y., Rangel, C., Reynolds, M. M., Caldwell, M. C., Johns, M., Nayak, M., Welsh, C. J. R., McDermott, S. and Datta, S. (2002) *Dev. Biol*. **253**, 247–257
35. Rubin, J. B., Choi, Y. and Segal, R. A. (2002) *Development* **129**, 2223–2232
36. Couchman, J. R. (2003) *Nat. Rev. Mol. Cell Biol*. **4**, 926-937
37. Fowlkes, J. L., Thrailkill, K. M., George-Nascimento, C., Rosenberg, C. K. and Serra, D. M. (1997) *Endocrinology* **138**, 2280-2285
38. Chan, J. A., Balasubramanian, S., Witt, R. M., Nazemi, K. J., Choi, Y., Pazyra-Murphy, M. F., Walsh, C. O., Thompson M. and Segal, R. A. (2009) *Nat. Neurosci*. **12**, 409-417
39. Vyas, N., Goswami, D., Manonmani, A., Sharma, P., Ranganath, H.A., VijayRaghavan, K., Shashidhara, L.S., Sowdhamini, R. and Mayor, S. (2008) *Cell* **133**, 1214-1337
40. Gallet, A., Staccini-Lavenant, L. and Thérond, P.P. (2008) *Dev. Cell* **14**, 712-725
41. Molofsky, A. V., Pardal, R., Iwashita, T., Park, I. K., Clarke, M. F. and Morrison, S. J. (2003) *Nature* **425**,962–967
42. Pardal, R.,Molofsky, A. V., He, S. and Morrison, S. J. (2005) *Cold Spring Harb. Symp. Quant. Biol.* **70**,177–185
43. Capurro, M. I., Xu, P., Shi, W., Li, F., Jia, A. and Filmus, J. (2008) *Dev. Cell* **14**,700-711
44. Gallet, A., Staccini-Lavenant, L. and Thérond, P. P. (2008) *Dev. Cell* **14**,712-725

FOOTNOTES

We thank Drs. Marek Cebecauer, Hinke Multhaupt, Kay Grobe, Jane Srivastava, Abul Tarafder and Atsuko Yoneda for help with various aspects of the work and gifts of cells and reagents. JRC was supported by The Danish National Research Foundation, Lundbeck Fonden, Danish Medical Research Council and Fabrikant Vilhelm Pedersen og Hustrus Legat through Novo Nordisk Fonden. AIM was supported by Medical Research Council (UK) grant G007771.

Abbreviations used are: CF – carboxyfluorescein, CFSE – carboxyfluorescein, succinimidyl ester, FBS- fetal bovine serum, Hh – Hedgehog, MFI – mean fluorescence intensity, Shh – Sonic Hedgehog

FIGURE LEGENDS

FIGURE 1. Modelling of Heparin- Sonic Hedgehog (mShh) interactions.
The three lowest energy predictions for the the heparin-mShh interaction from docking calculations are shown, with the protein structure exactly overlaid. The proteins are shown as ribbon diagrams coded red for helix, blue for beta strand and grey for loops and sequences lacking secondary structure. Heparin molecules are shown in stick form, coloured by element: grey for carbon, red for oxygen, blue for nitrogen, yellow for sulphur and white for hydrogen. **A.** The predicted complex between mShh (1VHH.pdb) and a heparin undecasaccharide, with heparin interacting residues K39 and K179 shown in green stick form. **B.** The predicted complex between hShh (3M1N.pdb) and a heparin undecasaccharide, with heparin interacting residues R28, K32 and K34 shown as green sticks; K38 and K178 are shown as orange sticks.

FIGURE 2. Characterisation of purified wild type and mutant hShh proteins by heparin affinity chromatography. Each of the five purified Shh proteins were analyzed by Western blot (**A)** and dot blot **(B)** with two Shh antibodies, H160 and 5E1. The latter confirms that all mutant hShh proteins retain appropriate conformation. Heparin binding efficacy of all five proteins was determined by heparin-Sepharose chromatography **(C)** with a linear elution gradient of 0-0.7 M NaCl in phosphate buffer (2.7 mM KCl, 10 mM Na_2HPO_4, 1.8 mM KH_2PO_4, pH 7.4).

FIGURE 3. Differentiation of C3H10T1/2 Osteoblast Precursor Cells requires hShh with heparin-binding properties. C3H10T1/2 osteoblast precursor cells were cultured in the presence of wild type hShh and hShh mutants at 300-2000 ng/ml for 5 days **(A).** The relative amount of Shh-induced alkaline phosphatase activity was measured as described in Materials and Methods to determine biological activity of the morphogen. As a control, Shh-treated cells were incubated with 5E1 anti-Shh to demonstrate specificity of Shh-induced differentiation **(B).** Values are mean ± S.D., n=9 in each group, * p-value <0.001 compared to control group ShhNC24II, ** p-value <0.001 compared to 5E1 treatment group, ‡ p-value <0.01 compared to 5E1 treatment group.

FIGURE 4. Signaling in human PDAC cells is mediated optimally by Shh with heparin-binding properties. Expression of Ptc and Gli1 were examined by both RT-PCR and Western blot in PANC1 cells after treatment of cells with recombinant wild type and mutant hShh. The PCR analysis and immunoblotting data are shown in **A** and **C** respectively and are quantified in **B** and **D**. Values are mean ± S.D., n=9 in each group in RT-PCR experiments **(B)**, * p-value <0.0001 compared to untreated group. ‡ p-value <0.001 compared to ShhNC24II group. In Western blotting assay (**D**, n=4), * p-value <0.0001 compared to untreated group. ‡ p-value <0.001 compared to ShhNC24II group.

FIGURE 5. Mutant hShh proteins that lack heparin affinity promote lower levels of PANC1 cell proliferation. Both 5E1 blocking antibody treatment on Day 1 (5E1 D1) and siRNA depletion of endogenous Shh (Shh KD) confirmed that PANC1 proliferation is Shh responsive. 5E1 treatment on Day 4 (5E1 D4) was used to mimic *in vivo* RNAi KD kinetics. The maximum labeling was determined by treating cells with CFSE just before flow cytometer assessment. To study the effect of the wild type and mutant Shh proteins in PANC1 proliferation, 8 days after Shh siRNA transfection /hShh treatment, the cells were analyzed by flow cytometry. The Y-axis shows the level of CF intensity observed from

30,000 cells. The experiments were repeated three times in triplicate, and statistical significance was assessed with the two-tailed t test (**, P< 0.0001 compared to untreated group; ‡, P< 0.0001 compared to Shh KD group).

FIGURE 6. PANC1 cell invasion in response to hShh requires the morphogen to possess heparin-binding properties. To study the effect of wild type and mutant Shh proteins on PANC1 invasion, 72 h after Shhs treatment/RNAi transfection the cells were plated onto Matrigel invasion chambers for 24 h. Cells that migrated from the upper to the lower side of the filter were photographed **(A)** and counted with a light microscope (10 fields/filter, **B**). The experiments were repeated four times, and statistical significance was calculated with the two-tailed t test (*, P< 0.001 compared to untreated samples; ‡, P< 0.0001 compared to ShhNC24II/Shh KD samples).

FIGURE 7. Multimerization of hShh proteins is reduced in parallel with decreased heparin affinity. 72 h after RNAi transfection, PANC1 conditioned media were TCA precipitated and examined by Western blot for Shh **(A)**. To examine the ability of mutated hShh proteins to form multimers, endogenous Shh was depleted by 16 hr siRNA treatment. Ectopically expressed wild type or mutant hShh was achieved by cDNA transfection. After 48 h incubation, conditioned media were analyzed by gel filtration chromatography (Superdex 200 10/300 GL column). After TCA precipitation, each fraction was probed by Shh dot blot **(B)** The elution of molecular mass standards are shown across the top of the dotblot, in kD. Monomerization factor (%) = (Monomer / Monomer + Multimer) X 100%.

Figure 1A

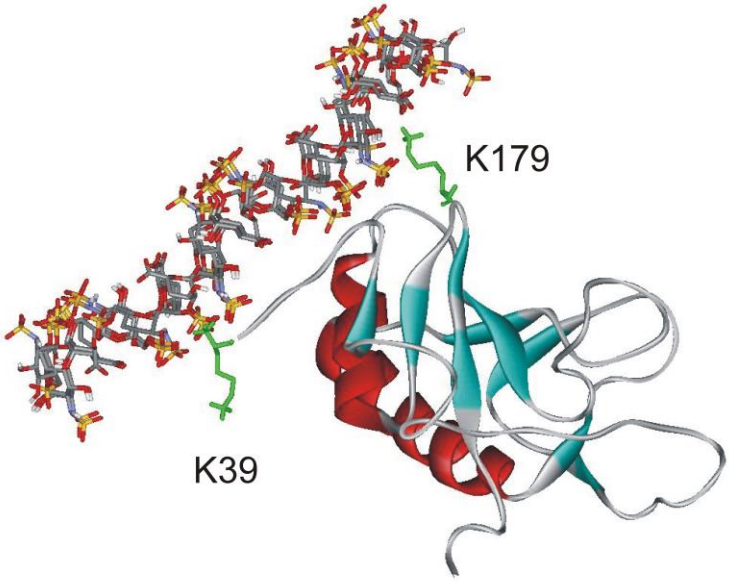


Figure 1B

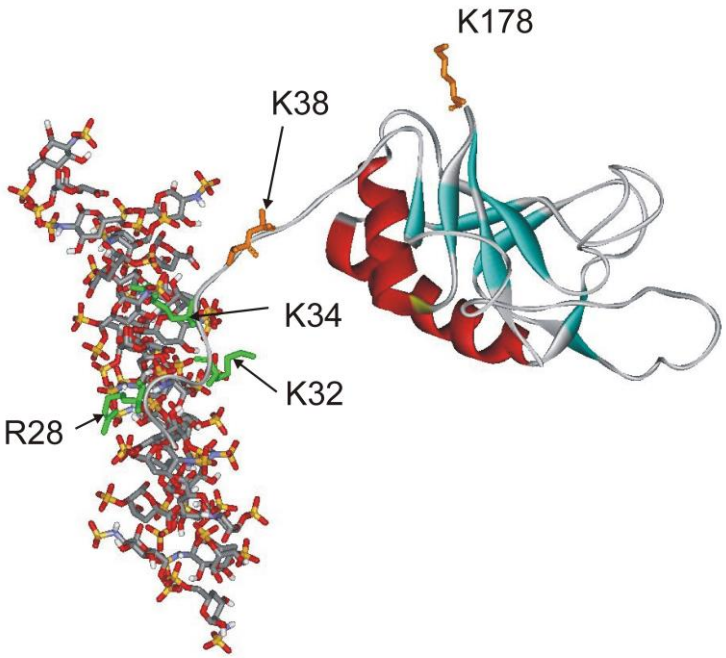


Figure 2.

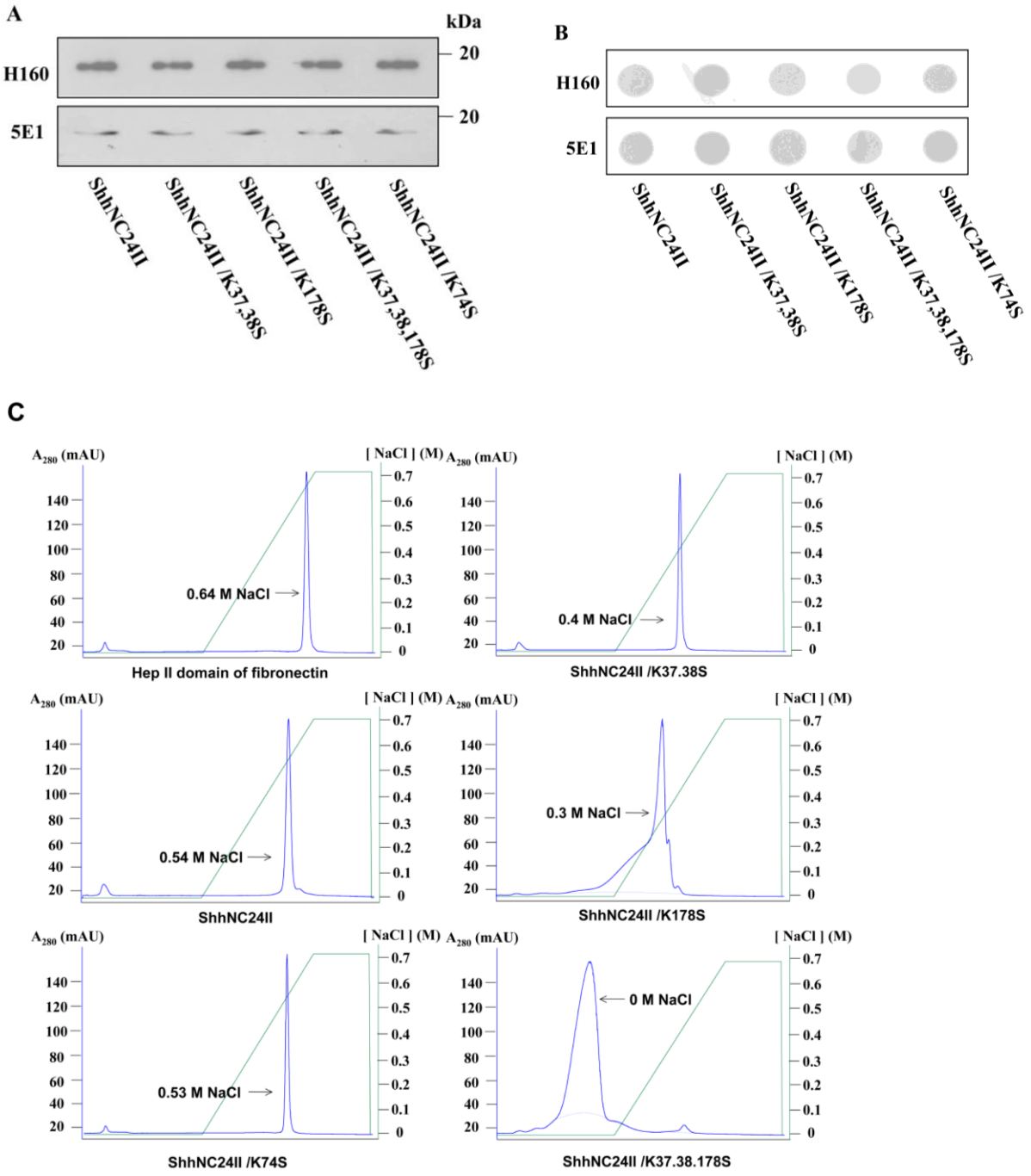

A
kDa
H160
5E1
20
20
ShhNC24II
ShhNC24II /K37,38S
ShhNC24II /K178S
ShhNC24II /K37,38,178S
ShhNC24II /K74S
B
H160
5E1
ShhNC24II
ShhNC24II /K37,38S
ShhNC24II /K178S
ShhNC24II /K37,38,178S
ShhNC24II /K74S
C
A280 (mAU)
[NaCl] (M)
0.64 M NaCl
Hep II domain of fibronectin
0.4 M NaCl
ShhNC24II /K37.38S
0.54 M NaCl
ShhNC24II
0.3 M NaCl
ShhNC24II /K178S
0.53 M NaCl
ShhNC24II /K74S
0 M NaCl
ShhNC24II /K37.38.178S

Figure 3.

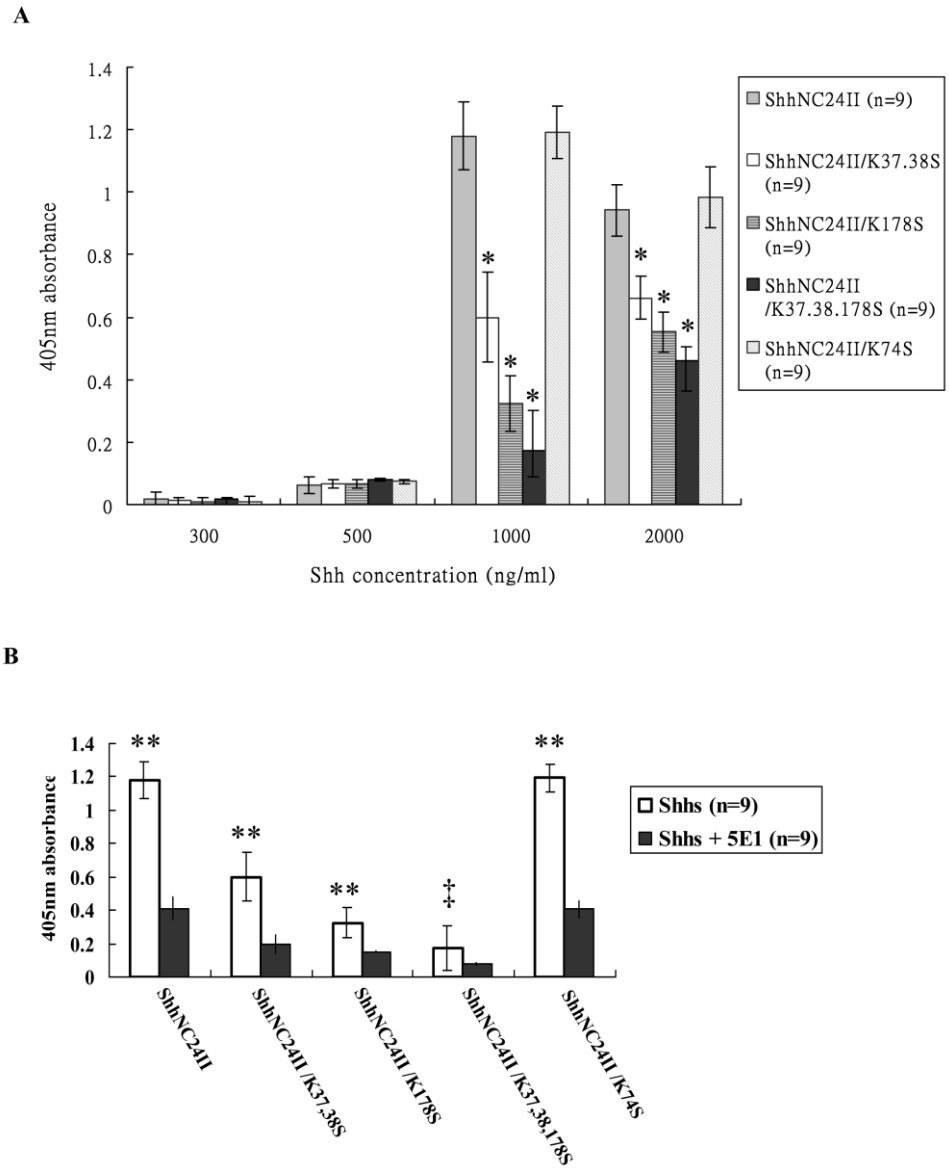
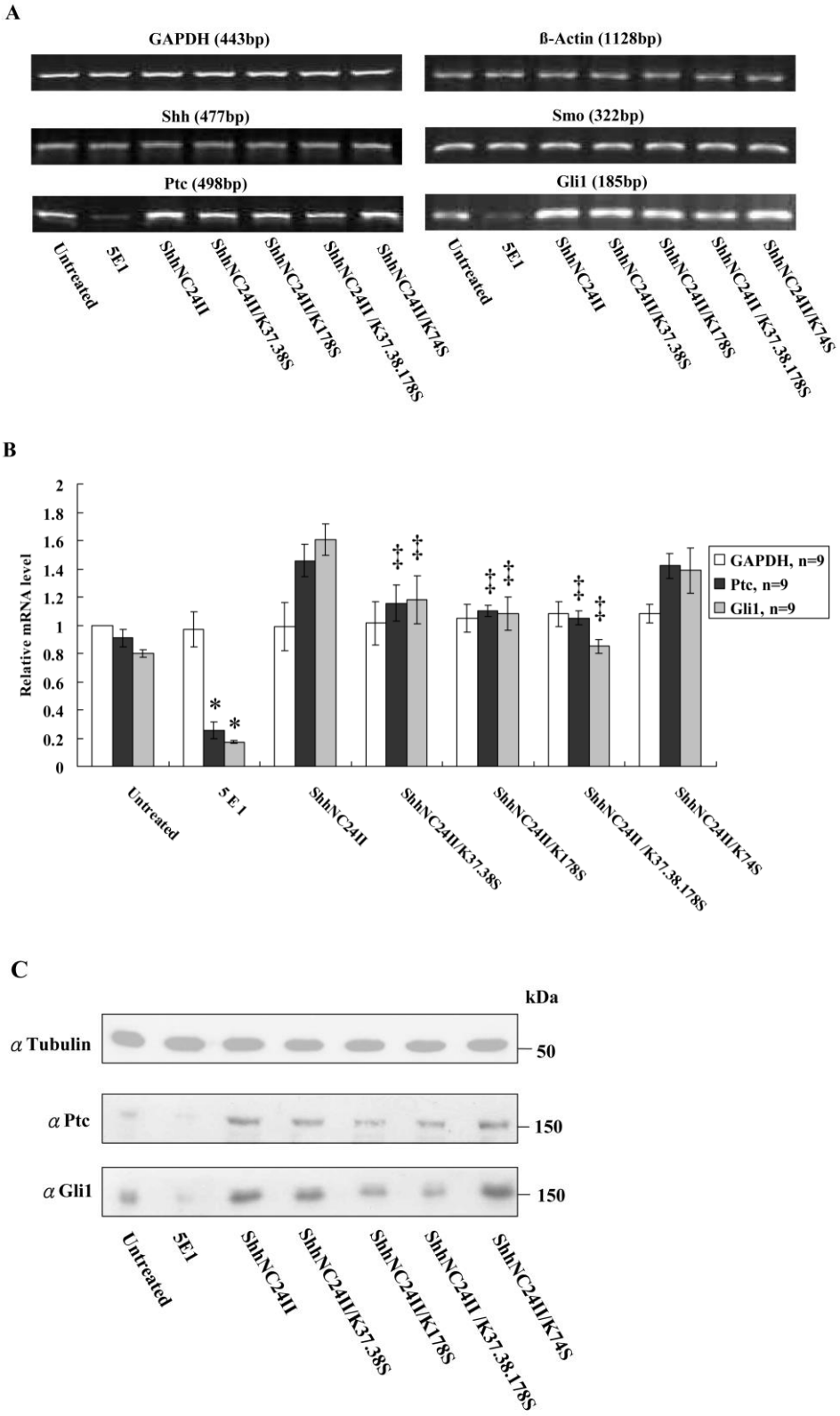

A
405nm absorbance
1.4
1.2
1
0.8
0.6
0.4
0.2
0
300
500
1000
2000
Shh concentration (ng/ml)
ShhNC24II (n=9)
ShhNC24II/K37.38S (n=9)
ShhNC24II/K178S (n=9)
ShhNC24II /K37.38.178S (n=9)
ShhNC24II/K74S (n=9)
B
405nm absorbance
Shhs (n=9)
Shhs + 5E1 (n=9)
ShhNC24II
ShhNC24II /K37.38S
ShhNC24II /K178S
ShhNC24II /K37.38.178S
ShhNC24II /K74S

Figure 4.


A
GAPDH (443bp)
ß-Actin (1128bp)
Shh (477bp)
Smo (322bp)
Ptc (498bp)
Gli1 (185bp)
Untreated
5E1
ShhNC24II
ShhNC24II/K37.38S
ShhNC24II/K178S
ShhNC24II /K37.38.178S
ShhNC24II/K74S
B
Relative mRNA level
GAPDH, n=9
Ptc, n=9
Gli1, n=9
C
kDa
α Tubulin
α Ptc
α Gli1
50
150
150

D

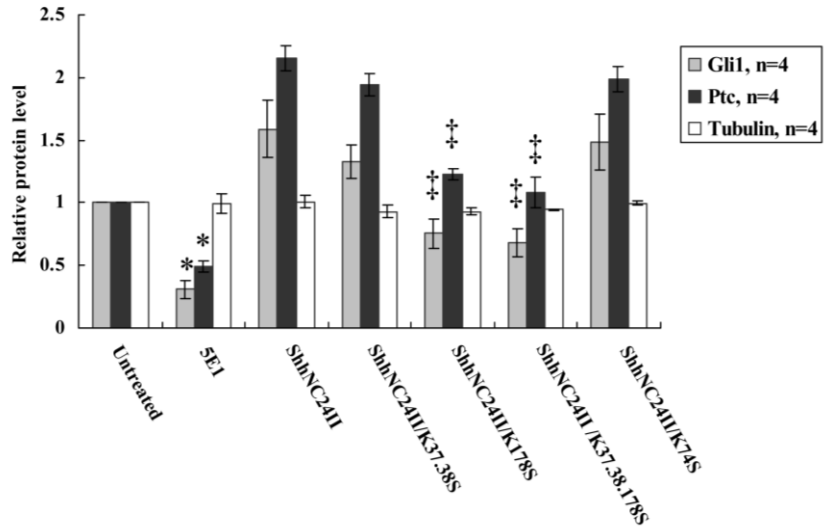

Relative protein level
2.5
2
1.5
1
0.5
0
Gli1, n=4
Ptc, n=4
Tubulin, n=4
Untreated
5E1
ShhNC24II
ShhNC24II/K37.38S
ShhNC24II/K178S
ShhNC24II /K37.38.178S
ShhNC24II/K74S

Figure 5.

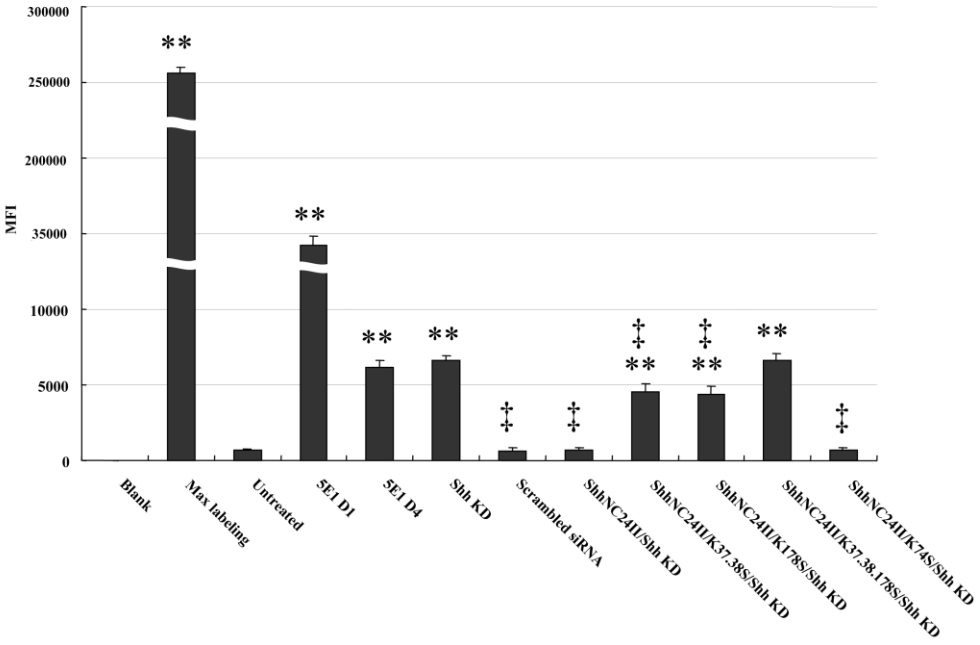
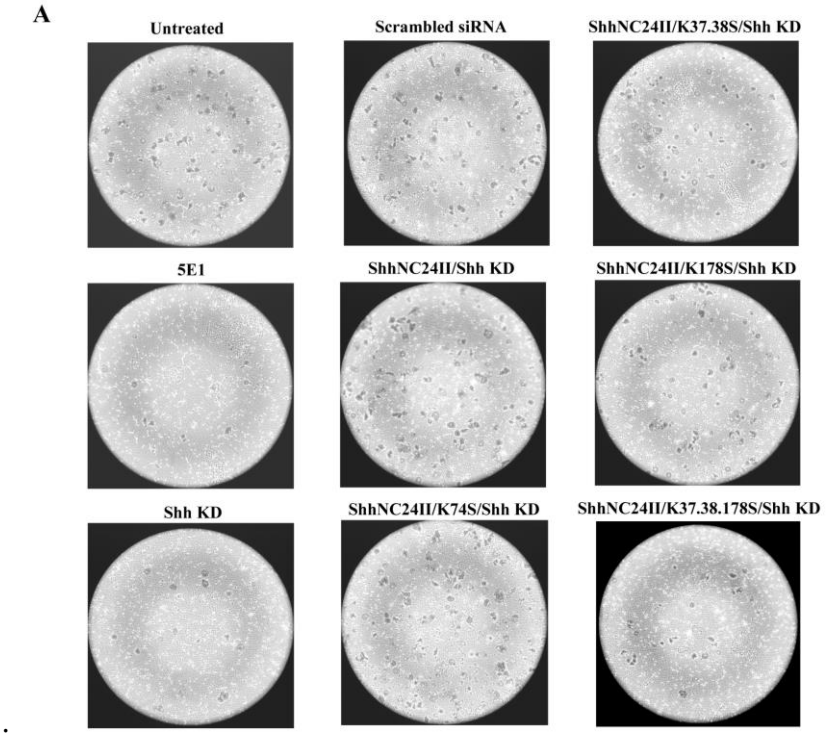

300000
250000
200000
35000
10000
5000
0
MFI
**
**
**
**
**
‡‡
**
‡‡
**
‡‡
**
‡
Blank
Max labeling
Untreated
5E1 D1
5E1 D4
Shh KD
Scrambled siRNA
ShhNC24II/Shh KD
ShhNC24II/K37.38S/Shh KD
ShhNC24II/K178S/Shh KD
ShhNC24II/K37.38.178S/Shh KD
ShhNC24II/K74S/Shh KD

Figure 6


A
Untreated
Scrambled siRNA
ShhNC24II/K37.38S/Shh KD
5E1
ShhNC24II/Shh KD
ShhNC24II/K178S/Shh KD
Shh KD
ShhNC24II/K74S/Shh KD
ShhNC24II/K37.38.178S/Shh KD

.

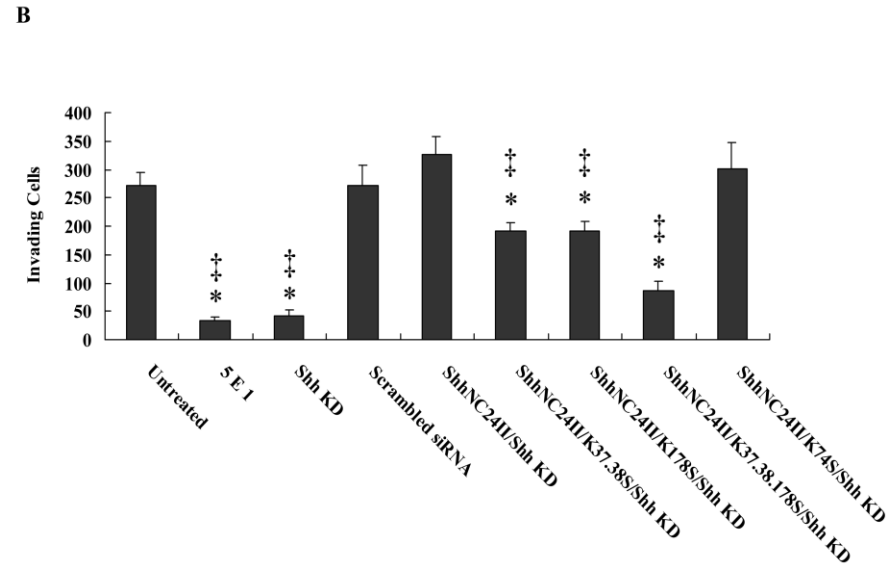
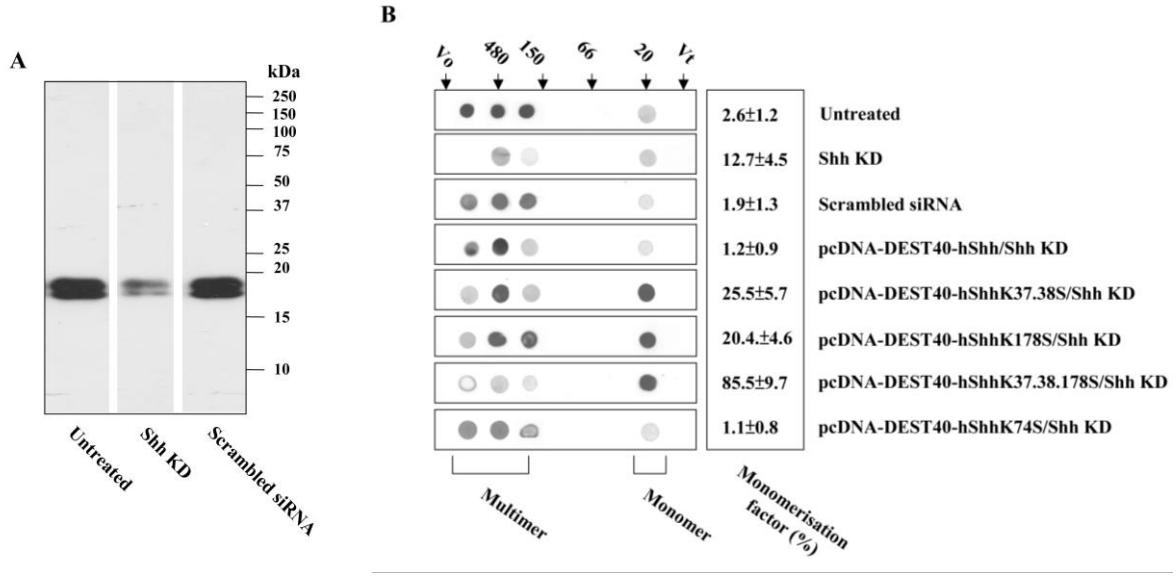

B
Invading Cells
400
350
300
250
200
150
100
50
0
Untreated
5E1
Shh KD
Scrambled siRNA
ShhNC24II/Shh KD
ShhNC24II/K37.38S/Shh KD
ShhNC24II/K178S/Shh KD
ShhNC24II/K37.38.178S/Shh KD
ShhNC24II/K74S/Shh KD

Figure 7.


A
kDa
250
150
100
75
50
37
25
20
15
10
Untreated
Shh KD
Scrambled siRNA
B
Vo
480
150
66
20
Vt
2.6±1.2
Untreated
12.7±4.5
Shh KD
1.9±1.3
Scrambled siRNA
1.2±0.9
pcDNA-DEST40-hShh/Shh KD
25.5±5.7
pcDNA-DEST40-hShhK37.38S/Shh KD
20.4.±4.6
pcDNA-DEST40-hShhK178S/Shh KD
85.5±9.7
pcDNA-DEST40-hShhK37.38.178S/Shh KD
1.1±0.8
pcDNA-DEST40-hShhK74S/Shh KD
Multimer
Monomer
Monomerisation factor (%)